Laser-field-induced modifications of electron-transfer processes in ion-atom collisions

Tom Kirchner*
Institut für Theoretische Physik, TU Clausthal, Leibnizstraße 10, D-38678 Clausthal-Zellerfeld, Germany
(Received 14 April 2004; published 21 June 2004)

Electron transfer in the presence of a laser field is explored for the prototype collision system He^{2+}-H(1*s*) on the basis of a quantum-mechanical calculation. At collision energies $E_P \geqslant 2$ keV/amu the capture probabilities are found to be conisderably enhanced or suppressed depending on the exact synchronization of the time-dependent projectile and laser interactions. At lower collision energies the total capture cross section is strongly enhanced irrespective of the relative phase between both fields. This enhancement should be directly observable in future experiments.

DOI: 10.1103/PhysRevA.69.063412 PACS number(s): 34.50.Rk, 32.80.Wr, 34.50.Fa, 34.70.+e

I. INTRODUCTION

Combined laser- and charged-particle induced electronic processes in atomic collisions are of considerable interest both from a fundamental and from a more applied point of view. First, they might broaden and deepen our general understanding of dynamic atomic processes, which has reached a certain maturity for laser-matter interactions and field-free collisions [1]. Second, and more specifically they might pave the way for the control of ultrashort quantum processes which are deemed to be important for a number of applications, such as laser-driven fusion, plasma heating, and the development of fast optical electronic devices.

The question to which extent electronic processes in ion-atom collisions can be modified and manipulated by suitable laser fields was first addressed some 25 years ago [2,3], but remained basically unanswered to the present date. The main reason for this situation is the absence of experimental data beyond thermal collision energies [4]. The theoretical results obtained in the 1970s and 1980s provided only modest insights into the physics and potentialities of laser-assisted collisions, since the models used were rather restrictive (cf. Ref. [5] and references therein). As the pilot studies were not followed by experimental investigations the activities in the field subsided over the years. Only recently has the development of advanced experimental and theoretical techniques triggered renewed attention and activities.

To date, scattering experiments within a laser field seem feasible and are being considered or planned in several laboratories. The main experimental challenge, the superposition of a laser beam, an energetic ion or electron beam, and a target has been mastered very recently [6]. The possible control of slow *atom*-atom collisions by laser light has been demonstrated with a somewhat different setup [7]. On the theoretical side refined methods for the description of laser-assisted collisions have been worked out, implemented and tested on prototype scattering systems. These works include perturbative calculations of electron capture [8–10] and ionization cross sections [11–13] in fast collisions assisted by relatively weak fields of low frequency, classical simulations of laser-assisted ionization events [14], and quantum-mechanical calculations for excitation, ionization [14,15], electron capture [5,16], and high harmonic generation [17] within more intense fields. All these works predict significant modifications of collisional or laser-induced processes when both types of interactions are combined.

The present paper elaborates on a pilot study of capture and ionization processes in He^{2+}-H collisions at impact energies in the keV range assisted by laser fields of moderate intensity and frequencies from the optical to the ultraviolet regime [5]. The time-dependent Schrödinger equation (TDSE) is solved using the basis generator method (BGM) [18,19], which has been rather successful for the description of field-free ion-atom collisions [20]. The adaptation of the BGM to the problem at hand is described in Sec. II. In Sec. III results for electron transfer are presented, and their implications for possible experimental investigations are discussed. Some concluding remarks are provided in Sec. IV. Atomic units ($\hbar = m_e = e = 1$) are used unless stated otherwise.

II. THEORY

Laser-assisted ion-atom collisions at not too low collision energies and field intensities can be described semiclassically, i.e., projectile and laser interactions can be taken into account in terms of time-dependent external potentials which govern the quantum dynamics of the electrons. In the present work the projectile is assumed to move on a straight-line trajectory $\mathbf{R}(t) = (b, 0, v_P t)$ with impact parameter b and collision velocity v_P. The laser interaction in length gauge and dipole approximation is characterized by the oscillating electric field

$$\mathbf{E}(t) = \epsilon_{\rm pol} E_0 \sin(\omega t + \delta) \tag{1}$$

with constant amplitude E_0, frequency ω, initial phase δ, and a polarization vector $\epsilon_{\rm pol}$ of unit length. For a one-electron problem the nonrelativistic Hamiltonian takes the form

$$\hat{H}(t) = -\frac{1}{2}\Delta - \frac{Q_T}{r} - \frac{Q_P}{|\mathbf{r} - \mathbf{R}(t)|} - \mathbf{r}\cdot\mathbf{E}(t), \tag{2}$$

where Q_T and Q_P are the charges of the target and the projectile nuclei, respectively. We have to solve the TDSE,

*Electronic address: tom.kirchner@tu-clausthal.de

$$i\partial_t|\Psi(t)\rangle = \hat{H}(t)|\Psi(t)\rangle, \tag{3}$$

for the hydrogen ground state as initial condition $|\Psi(t_0)\rangle = |\phi_{1s}\rangle$. This is done by expanding $|\Psi(t)\rangle$ in a finite basis obtained from the BGM [18,19]. The BGM is built on the insight that convergence of a basis does not imply that one has to make an attempt at a complete representation of Hilbert space $\mathcal{H}$, but that one has to ensure that couplings to that part of $\mathcal{H}$ which is not covered by the basis are negligible. This can be achieved even with relatively modest basis sizes if the model space defined by the basis has the flexibility to adapt to the time development of the state vector $|\Psi(t)\rangle$.

The BGM starts with a finite set of eigenstates of the undisturbed system, i.e., in our case with a set of bound hydrogenic orbitals,

$$\hat{H}_0|\phi_v^0\rangle = \varepsilon_v|\phi_v^0\rangle, \quad v = 1, \ldots, V,$$

$$\hat{H}_0 = -\frac{1}{2}\Delta - \frac{Q_T}{r}, \tag{4}$$

which is called the *generating basis*. Successive mapping of these states with the Schrödinger operator $\hat{O} = \hat{H}(t) - i\partial_t$ generates a hierarchy of V-dimensional subspaces of $\mathcal{H}$,

$$|\phi_v^u(t)\rangle = \hat{O}|\phi_v^{u-1}(t)\rangle = \hat{O}^u|\phi_v^0\rangle, \quad v = 1, \ldots, V, \quad u = 1, \ldots, U \tag{5}$$

with the following properties: (i) the set of states $\{|\phi_v^u(t)\rangle, v = 1, \ldots, V; u = 0, \ldots, U\}$ is linearly independent and forms a $[V \times (U+1)]$-dimensional subspace $\mathcal{A}^{UV}$ of $\mathcal{H}$; (ii) for $u < U$ the states of Eq. (5) interact merely *within* the hierarchy of finite subspaces. Only the states which belong to the Uth subset couple to the infinite complementary space of $\mathcal{A}^{UV}$. If these states are not accessed during the time propagation, the TDSE is solved exactly in $\mathcal{A}^{UV}$ [18].

The structure of the states defined by Eq. (5) becomes rather involved with increasing order u. For a given time-dependent interaction $\hat{V}(t) \equiv \hat{H}(t) - \hat{H}_0$ it is thus useful to introduce an alternative set of states $\{|\chi_\nu^\mu(t)\rangle, \nu = 1, \ldots, N, \mu = 0, \ldots, M\}$ via the simpler ansatz

$$|\chi_\nu^\mu(t)\rangle = \hat{V}(t)^\mu|\chi_\nu^0\rangle, \tag{6}$$

thereby generating a second finite model space $\mathcal{R}^{MN}$. It can be shown [19] that for any given U, V there exist finite numbers $M(U,V)$ and $N(U,V)$ such that $\mathcal{A}^{UV} \subseteq \mathcal{R}^{MN}$ if two conditions are met: (i) the generating basis of Eq. (4) (including the physical initial condition) is contained in $\mathcal{R}^{0N}$; (ii) the operator $\hat{O}$ maps each state $|\chi_\nu^\mu(t)\rangle$ onto a *finite* linear combination $\mathcal{L}_{\mu\nu}$ of the states $\{|\chi_\lambda^\kappa(t)\rangle\}$,

$$\hat{O}|\chi_\nu^\mu(t)\rangle = \mathcal{L}_{\mu\nu}(\{|\chi_\lambda^\kappa(t)\rangle\}) \in [|\chi_\lambda^\kappa(t)\rangle, \lambda = 1, \ldots, L, \kappa = 0, \ldots, K], \tag{7}$$

where $L = L(\mu, \nu)$ and $K = K(\mu, \nu)$.

For the field-free two-center Coulomb problem such a basis can be found if one regularizes the potentials according to

$$V_T = -\frac{Q_T}{r} \to -\frac{Q_T}{[r^2 + \epsilon_T^2]^{1/2}} = -Q_T W_T(\epsilon_T),$$

$$V_P(t) = -\frac{Q_P}{r_P(t)} \to -\frac{Q_P}{[r_P^2(t) + \epsilon_P^2]^{1/2}} = -Q_P W_P(t, \epsilon_P) \tag{8}$$

with $r_P(t) = |\mathbf{r} - \mathbf{R}(t)|$. The parameters ϵ_T, ϵ_P can be interpreted as nuclear radii which are small but finite. In Ref. [19] we proved that the set of states

$$\chi_{nlm}^0(\mathbf{r}, \xi, \epsilon_T) = r_{\epsilon_T}^{n-1}\exp(-\xi r_{\epsilon_T})(r/r_{\epsilon_T})^l Y_l^m(\theta, \varphi),$$

$$\chi_{nlm}^\mu(\mathbf{r}, t, \xi, \epsilon_T, \epsilon_P) = [W_P(t, \epsilon_P)]^\mu \chi_{nlm}^0(\mathbf{r}, \xi, \epsilon_T) \tag{9}$$

with $r_{\epsilon_T} = [r^2 + \epsilon_T^2]^{1/2}$ and

$$l, \mu, L, N, M \in \mathcal{N}_0, \quad m, n, N_z \in \mathcal{Z},$$

$$-l \leqslant m \leqslant l \leqslant L, \quad l + N_z < n \leqslant N,$$

$$N_z \leqslant 0 \leqslant L \leqslant N - 1, \quad 0 \leqslant \mu \leqslant M \tag{10}$$

fulfills the above-mentioned conditions rigorously. The very same BGM basis (9) fulfills those conditions also for the Hamiltonian (2) of *laser-assisted* collisions, since the laser potential in Eq. (2) maps each BGM state onto a finite linear combination of BGM states. This is demonstrated in the Appendix.

Numerous applications of the BGM have shown that the numerically simpler ansatz

$$\tilde{\chi}_{nlm}^\mu(\mathbf{r}, t, \alpha) = [\tilde{W}_P(t, \alpha)]^\mu \phi_{nlm}^0(\mathbf{r}), \tag{11}$$

where the set $\{\chi_{nlm}^0\}$ is replaced by a set of atomic orbitals $\{\phi_{nlm}^0\}$ defined by Eq. (4) and where the alternative regularization

$$\tilde{W}_P(t, \alpha) = \frac{1}{r_P}[1 - \exp(-\alpha r_P)] \tag{12}$$

with $\alpha = 1$ is used [18], has been rather successful for the description of field-free ion-atom collisions [20]. Therefore this approximate BGM basis is also employed for the present problem of laser-assisted collisions (cf. Ref. [5]), i.e., the state vector is expanded according to

$$|\Psi(t)\rangle = \sum_{\mu=0}^{M}\sum_{v=1}^{V} c_{\mu v}(t)|\tilde{\chi}_\mu^v(t)\rangle \tag{13}$$

and the set of coupled-channel equations

$$i\sum_{\mu=0}^{M}\sum_{v=1}^{V} \dot{c}_{\mu v}(t)\langle\tilde{\chi}_w^\lambda(t)|\tilde{\chi}_v^\mu(t)\rangle = \sum_{\mu=0}^{M}\sum_{v=1}^{V} c_{\mu v}(t)\langle\tilde{\chi}_w^\lambda(t)|\hat{H}(t) - i\partial_t|\tilde{\chi}_v^\mu(t)\rangle \tag{14}$$

is solved by standard methods. The basis used includes all atomic hydrogen states of the *KLMN* shells and 91 BGM states from the set $\{|\tilde{\chi}_v^\mu(t)\rangle, \mu = 1, \ldots, M = 8\}$. Electron cap-

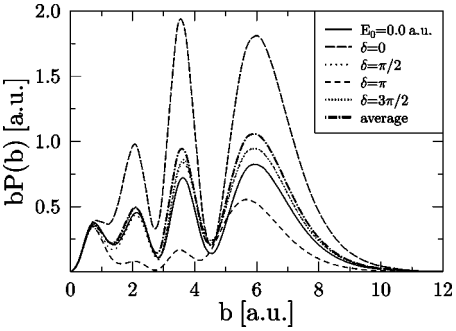

FIG. 1. Impact-parameter-weighted total capture probabilities as functions of the impact parameter for He^{2+}-H collisions at projectile energy $E_P=2$ keV/amu, laser field strength $E_0=0.02$ a.u., frequency $\omega=0.1$ a.u., and longitudinal polarization $\boldsymbol{\epsilon}_{\mathrm{pol}}\|\mathbf{v}_P$. Results for different initial phases δ, the phase average, and the field-free case are displayed.

ture is calculated by projecting the state vector onto all traveling projectile states $He^+(n=1,2,3)$ at a final time $t=t_f$ that corresponds to an internuclear distance of 45 a.u.

III. RESULTS

In Ref. [5] electron transfer in He^{2+}-H collisions at 2 keV/amu was studied in linearly polarized laser fields with the polarization vector $\boldsymbol{\epsilon}_{\mathrm{pol}}$ oriented parallel to the ion-beam axis ($\boldsymbol{\epsilon}_{\mathrm{pol}}\|\mathbf{v}_P$). The field amplitude $E_0=0.02$ a.u. (corresponding to the intensity $I=1.4\times10^{13}$ W/cm^3) and frequencies in the range from 0.01 to 1 a.u. (corresponding to wavelengths from 4560 to 45.6 nm) were chosen so that ionization in the absence of the projectile ion is small, i.e., well below 1% at t_f. While the calculations have been performed with a constant field amplitude E_0 it is noted that linearly ramped laser fields do not lead to different results in this paramter range. It was found for frequencies below $\omega\approx0.3$ a.u. that the total capture cross section depends crucially on the phase δ of the oscillating electric field [cf. Eq. (1)]. The variations as a function of δ maximize at frequencies around $\omega=0.1$ a.u. with strongly enhanced and suppressed capture for $\delta=0$ and $\delta=\pi$, respectively. The phase-averaged capture was found to be remarkably constant in the frequency range below $\omega=0.3$ a.u. exhibiting an approximate 30% enhancement of the field-free cross section.

These findings are further illustrated by Fig. 1. Phase-dependent impact-parameter-weighted capture probabilities at $\omega=0.1$ a.u. are compared with the phase-averaged curve and the field-free result, which is in close agreement with state-of-the-art calculations (cf. Fig. 1 of Ref. [21]). Similarly to the case of $\omega=0.2$ a.u. which was discussed in Ref. [5] the capture probabilities at $\delta=0$ and $\delta=\pi$ are strongly enhanced or suppressed while $\delta=\pi/2$ and $\delta=3\pi/2$ do not yield significant effects.

It was argued in Ref. [5] that these variations can be understood by considering the expectation value $z_e(t)\equiv\langle\Psi(t)|z|\Psi(t)\rangle$ of the electronic coordinate in the longitudinal direction. This is demonstrated in Fig. 2 for the impact parameter $b=5.8$ a.u. for which the weighted capture prob-

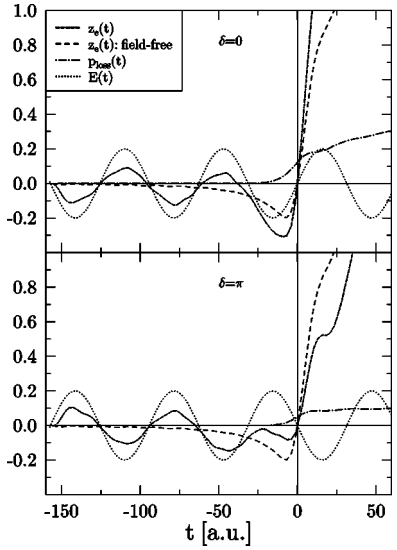

FIG. 2. Time development of the laser field $E(t)$ (in a.u. multiplied by a factor of 10), the electron loss probability $p_{\mathrm{loss}}(t)$, and the expectation value $z_e(t)\equiv\langle\Psi(t)|z|\Psi(t)\rangle$ (in a.u.) for He^{2+}-H collisions at projectile energy $E_P=2$ keV/amu, impact parameter $b=5.8$ a.u., laser field strength $E_0=0.02$ a.u., frequency $\omega=0.1$ a.u., and longitudinal polarization $\boldsymbol{\epsilon}_{\mathrm{pol}}\|\mathbf{v}_P$.

ability exhibits a pronounced maximum (cf. Fig. 1). The expectation values for $\delta=0$ and $\delta=\pi$ are plotted along with the oscillating laser field (1) and the total electron loss, i.e., the sum of the (dominant) capture and the (small) ionization contributions. In the incoming channel ($t<0$) the laser field gives rise to oscillations of the electron cloud while the approaching projectile polarizes the density distribution along the negative z direction. For the case $\delta=0$ both time-dependent fields are synchronized such that they conspire and elongate the electron cloud stronger in the negative and positive z directions than the projectile alone before and after the closest approach at $t=0$. As a result of this "concerted action" capture is enhanced. If one chooses $\delta=\pi$ the laser field opposes the projectile field around the closest approach, and capture is reduced.

Apparently, this phase dependence is a dynamical effect which allows one, in principle, to manipulate the population of the final states rather profoundly. While such fine tuning seems unrealizable experimentally it might be possible to observe fingerprints of the (anti-)synchronization of laser and ion fields in highly differential spectra, since subfemtosecond phase information is accesible via the drift momentum of the recoiling target ion [22].

The enhancement of the phase-averaged capture cross section should be observable directly. It is therefore in order to check whether this effect is more prominent in other parameter regions. To this end extensive calculations have been performed as functions of collision velocity and laser frequency, but at fixed field strength $E_0=0.02$ a.u. As a general result it is found that the phase-averaged capture approaches the field-free result towards faster collisions while more pronounced differences are observed at lower velocities. This is demonstrated in Figs. 3 and 4, which display impact-parameter-weighted capture probabilities at $E_P=1$ keV/amu and $E_P=0.25$ keV/amu.

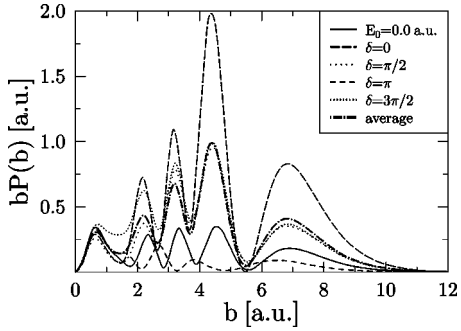

FIG. 3. Impact-parameter-weighted total capture probabilities as functions of the impact parameter for He^{2+}-H collisions at projectile energy $E_P=1$ keV/amu, laser field strength $E_0=0.02$ a.u., frequency $\omega=0.1$ a.u., and longitudinal polarization $\epsilon_{\rm pol}\|\mathbf{v}_P$. Results for different initial phases δ, the phase average, and the field-free case are displayed.

At $E_P=1$ keV/amu the phase sensitivity is even more pronounced than at $E_P=2$ keV/amu (Fig. 1), while the phase-averaged result is enhanced by more than a factor of 2 compared to 30% at $E_P=2$ keV/amu. At $E_P=0.25$ keV/amu field-free capture is very small, which is due to the fact that the collision system with doubly charged projectile and singly charged target nuclei is asymmetric, and energy is needed to induce transitions between the relevant molecular states [for a correlation diagram of the $(HHe)^{2+}$ system see, e.g., Ref. [23]]. By contrast, field-assisted capture is very efficient for all phases δ. At even lower projectile energies the phase dependence vanishs completely as the field oscillations are fast compared to the slow ion movement in this region. Moreover, the inefficient field-free capture signals that the projectile potential itself exerts but a minor influence on the electron dynamics. It merely makes final states available which are populated due to the action of the laser field.

In order to gain a more comprehensive picture of the laser-induced enhancement total capture cross sections are shown in Fig. 5 as functions of the projectile energy. The field-free results are compared with experimental data [24,25] and with two state-of-the-art calculations based on

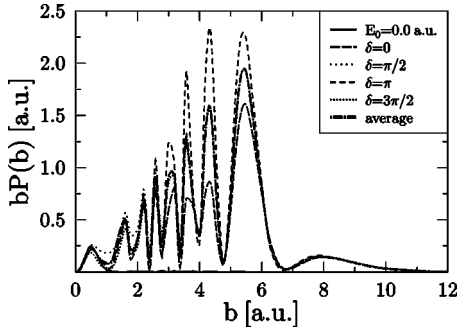

FIG. 4. Impact-parameter-weighted total capture probabilities as functions of the impact parameter for He^{2+}-H collisions at projectile energy $E_P=0.25$ keV/amu, laser field strength $E_0=0.02$ a.u., frequency $\omega=0.1$ a.u., and longitudinal polarization $\epsilon_{\rm pol}\|\mathbf{v}_P$. Results for different initial phases δ, the phase average, and the field-free case are displayed.

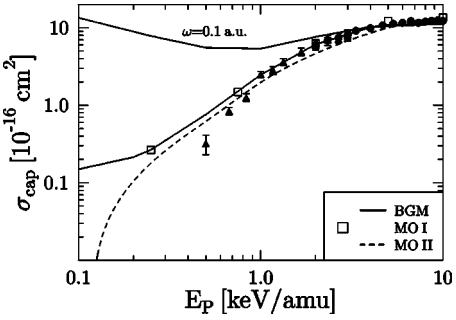

FIG. 5. Total capture cross sections as functions of impact energy for He^{2+}-H collisions. BGM results for field-free and phase-averaged laser-assisted collisions at field strength $E_0=0.02$ a.u., frequency $\omega=0.1$ a.u., and longitudinal polarization $\epsilon_{\rm pol}\|\mathbf{v}_P$. MO I: molecular-orbital calculation of Ref. [23]; MO II: molecular-orbital calculation of Ref. [26]. Experiments: circles [24], triangles [25].

molecular expansions [23,26]. Detailed comparisons with other theoretical (and experimental) data can be found in the latter works and in Refs. [21,27]. We observe good agreement with the present calculation except for very low projectile energies where the results of Ref. [26] decrease much more steeply. The reason for this behavior is that a curved instead of a straight-line trajectroy was used in Ref. [26] to describe the nuclear motion. In very slow field-free collisions, capture occurs only at small internuclear distances (cf. Fig. 4), which are, however, supressed by the Coulomb repulsion. The semiclassical approximation itself was shown to be valid down to $E_P\approx 0.1-0.2$ keV/amu. Only below these energies did quantum-mechanical calculations based on a partial wave expansion yield results that differed substantially from the semiclassical ones based on curved trajectories [26].

The phase-averaged laser-assisted capture cross section at $\omega=0.1$ a.u. exceeds the field-free result by orders of magnitude at low collision energies. This dramatic enhancement should be easily observable in experiments. One can expect that curved trajectories will not change the field-assisted cross section significantly even at the lowest energies shown as the dominant contributions are due to relatively large impact parameters (cf. Fig. 4) where the Coulomb repulsion of the nuclei is small. However, this claim should be corroborated by future calculations.

Finally, the frequency dependence of the field-assisted phase-averaged capture cross section is studied in Fig. 6. The strongest enhancement is found around $\omega=0.1$ a.u. for the lowest collision energy. A qualitatively similar behavior was observed in an early study of laser-assisted capture in He^{2+}-H collisions, albeit at lower field intensities and even lower projectile velocities [28]. That work was based on an approximate two-state molecular treatment, in which laser-assisted capture occurs as a consequence of couplings between the relevant quasimolecular states induced by the laser potential. One might expect that the cross section maximizes if one chooses the laser frequency such that it matches the energy difference between the quasimolecular states at the internuclear distance where the coupling matrix element is largest [29]. For the He^{2+}-H collision system this resonance condition yields $\omega\approx 0.15$ a.u. as optimal frequency. How-

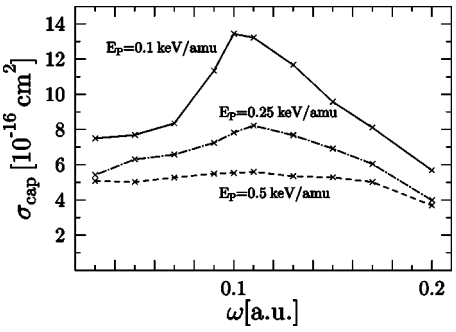

FIG. 6. Total capture cross sections as functions of laser frequency for He^{2+}-H collisions. BGM results for phase-averaged laser-assisted collisions at field strength $E_0=0.02$ a.u., different projectile energies E_P, and longitudinal polarization $\epsilon_{\mathrm{pol}}\|\mathbf{v}_P$.

ever, the authors of Ref. [28] found the largest capture cross section around $\omega=0.1$ a.u., in accord with the present results. This indicates that the relatively crude model of Ref. [28] includes the relevant physics at very low collision energies, but that a naive prediction based on correlation diagrams and coupling matrix elements alone is not sufficient to describe the situation.

With increasing energy the cross section curves displayed in Fig. 6 flatten and the phase-averaged capture becomes practically independent of the frequency (cf. Fig. 2 in Ref. [5]). As demonstrated above it is only in this region that the projectile potential is strong enough to induce appreciable electronic transitions. At the same time its synchronization with the oscillating laser field gains importance, and the simultaneous action of both fields either enhances or suppresses capture such that on average the laser effects decrease and the field-free result is approached.

IV. CONCLUDING REMARKS

Electron capture in slow ion-atom collisions is considerably modified when the collision is embedded in a laser field. The present calculations for $He^{2+}-H$ collisions confirm the prediction of early works [2,28] that the total capture cross section in an asymmetric collision system can be enhanced by orders of magnitude at very low impact energies where field-free capture is weak. This enhancement should be directly observable, and it is therefore suggested that future experiments concentrate at first on this region. At somewhat higher impact energies field-free capture is stronger and the laser effects become more subtle. A truly dynamical effect which depends on the synchronization of laser and projectile interactions is observed in this region. If one could control the fields on a time scale well below one optical cycle one could use this effect to control the electron dynamics, i.e., one could either enhance or suppress the capture probability significantly by choosing appropriate relative phases. Such fine tuning seems unrealizable at present, but it might be possible to observe fingerprints of the synchronization of the fields in highly differential measurements.

From the theoretical perspective these findings imply that in general one cannot content oneself with a calculation for a single phase. Instead, one has to consider all relative phases of the two external fields in order to obtain a complete picture of the collision dynamics. This makes such calculations relatively costly.

It is of interest to extend the calculations to other polarization directions relative to the ion beam axis, as well as to circularly polarized fields, for which circular dichroism has been suggested to play a visible role [30]. Moreover, the present approach can also be used to study ionization and excitation processes in field-assisted collisions [5], and can be extended to the investigation of many-electron systems within the framework of density-functional theory [31,32]. While interesting results can be expected from such purely theoretical works experimental efforts are necessary and highly desirable to foster laser-assisted collisions and help establish a lively subfield of modern atomic collision physics.

ACKNOWLEDGMENT

It is a pleasure to thank Hans Jürgen Lüdde for many useful discussions and his continuous encouragement to do this work.

APPENDIX

We have to show that the laser interaction in the Hamiltonian (2) maps each BGM state (9) onto a *finite* linear combination of BGM states. The laser potential in length gauge and dipole approximation is a scalar product of the position vector $\mathbf{r}$ of the electron and the polarization vector ϵ_{pol} multiplied by a merely time-dependent function [cf. Eq. (1)]. In order to prove the BGM condition for all polarizations (linear and elliptical) we have to evaluate the expressions $x_i\chi^0_{nlm}(\mathbf{r},\xi,\epsilon_T)$ for the three Cartesian components,

$$x\chi^0_{nlm}(\mathbf{r},\xi,\epsilon_T) = r^{\,l+1} r_{\epsilon_T}^{\,n-l-1}\exp(-\xi r_{\epsilon_T})\sin\theta\cos\varphi Y_l^m(\theta,\varphi),$$

$$y\chi^0_{nlm}(\mathbf{r},\xi,\epsilon_T) = r^{\,l+1} r_{\epsilon_T}^{\,n-l-1}\exp(-\xi r_{\epsilon_T})\sin\theta\sin\varphi Y_l^m(\theta,\varphi),$$

$$z\chi^0_{nlm}(\mathbf{r},\xi,\epsilon_T) = r^{\,l+1} r_{\epsilon_T}^{\,n-l-1}\exp(-\xi r_{\epsilon_T})\cos\theta Y_l^m(\theta,\varphi). \tag{A1}$$

Using the abbreviation $\kappa=\cos\theta$, the relation

$$Y_l^m(\theta,\varphi) = \sqrt{\frac{2l+1}{4\pi}\frac{(l-m)!}{(l+m)!}}P_l^m(\kappa)\exp(im\varphi) \tag{A2}$$

and the recursion formulas for the associated Legendre functions [33],

$$\kappa P_l^m(\kappa) = \frac{1}{2l+1}[(l-m+1)P_{l+1}^m(\kappa) + (l+m)P_{l-1}^m(\kappa)], \tag{A3}$$

$$\sqrt{1-\kappa^2}P_l^m(\kappa) = \frac{1}{2l+1}[P_{l-1}^{m+1}(\kappa) - P_{l+1}^{m-1}(\kappa)] \tag{A4}$$

$$= \frac{1}{2l+1}[(l-m+1)(l-m+2)P_{l+1}^{m-1}(\kappa) - (l+m)(l+m-1)P_{l-1}^{m-1}(\kappa)], \tag{A5}$$

which hold for positive and negative values of m if the convention

$$P_l^{-m}(\kappa) = (-1)^m \frac{(l-m)!}{(l+m)!}P_l^m(\kappa) \tag{A6}$$

is used, we obtain for the angular parts in Eq. (A1)

$$\sin\theta\cos\varphi Y_l^m(\theta,\varphi) = -\frac{1}{2}\left(\sqrt{\frac{(l+m+1)(l+m+2)}{(2l+1)(2l+3)}}Y_{l+1}^{m+1}(\theta,\varphi) - \sqrt{\frac{(l-m+1)(l-m+2)}{(2l+1)(2l+3)}}Y_{l+1}^{m-1}(\theta,\varphi)\right.$$
$$\left. - \sqrt{\frac{(l-m-1)(l-m)}{(2l-1)(2l+1)}}Y_{l-1}^{m+1}(\theta,\varphi) + \sqrt{\frac{(l+m-1)(l+m)}{(2l-1)(2l+1)}}Y_{l-1}^{m-1}(\theta,\varphi)\right) \tag{A7}$$

$$\sin\theta\sin\varphi Y_l^m(\theta,\varphi) = \frac{i}{2}\left(\sqrt{\frac{(l+m+1)(l+m+2)}{(2l+1)(2l+3)}}Y_{l+1}^{m+1}(\theta,\varphi) + \sqrt{\frac{(l-m+1)(l-m+2)}{(2l+1)(2l+3)}}Y_{l+1}^{m-1}(\theta,\varphi)\right.$$
$$\left. - \sqrt{\frac{(l-m-1)(l-m)}{(2l-1)(2l+1)}}Y_{l-1}^{m+1}(\theta,\varphi) - \sqrt{\frac{(l+m-1)(l+m)}{(2l-1)(2l+1)}}Y_{l-1}^{m-1}(\theta,\varphi)\right), \tag{A8}$$

$$\cos\theta Y_l^m(\theta,\varphi) = \sqrt{\frac{(l-m+1)(l+m+1)}{(2l+1)(2l+3)}}Y_{l+1}^m(\theta,\varphi) + \sqrt{\frac{(l-m)(l+m)}{(2l-1)(2l+1)}}Y_{l-1}^m(\theta,\varphi). \tag{A9}$$

If we furthermore take into account that $r^2 = r_{\epsilon_T}^2 - \epsilon_T^2$ we finally obtain

$$x\chi_{nlm}^{\mu}(\mathbf{r},t,\xi,\epsilon_T,\epsilon_P) = -\frac{1}{2}\left(\sqrt{\frac{(l+m+1)(l+m+2)}{(2l+1)(2l+3)}}\chi_{(n+1)(l+1)(m+1)}^{\mu}(\mathbf{r},t,\xi,\epsilon_T,\epsilon_P)\right.$$
$$- \sqrt{\frac{(l-m+1)(l-m+2)}{(2l+1)(2l+3)}}\chi_{(n+1)(l+1)(m-1)}^{\mu}(\mathbf{r},t,\xi,\epsilon_T,\epsilon_P)$$
$$- \sqrt{\frac{(l-m-1)(l-m)}{(2l-1)(2l+1)}}[\chi_{(n+1)(l-1)(m+1)}^{\mu}(\mathbf{r},t,\xi,\epsilon_T,\epsilon_P) - \epsilon_T^2\chi_{(n-1)(l-1)(m+1)}^{\mu}(\mathbf{r},t,\xi,\epsilon_T,\epsilon_P)]$$
$$\left. + \sqrt{\frac{(l+m-1)(l+m)}{(2l-1)(2l+1)}}\chi_{(n+1)(l-1)(m-1)}^{\mu}(\mathbf{r},t,\xi,\epsilon_T,\epsilon_P) - \epsilon_T^2\chi_{(n-1)(l-1)(m-1)}^{\mu}(\mathbf{r},t,\xi,\epsilon_T,\epsilon_P)\right),$$

$$y\chi_{nlm}^{\mu}(\mathbf{r},t,\xi,\epsilon_T,\epsilon_P) = \frac{i}{2}\left(\sqrt{\frac{(l+m+1)(l+m+2)}{(2l+1)(2l+3)}}\chi_{(n+1)(l+1)(m+1)}^{\mu}(\mathbf{r},t,\xi,\epsilon_T,\epsilon_P)\right.$$
$$+ \sqrt{\frac{(l-m+1)(l-m+2)}{(2l+1)(2l+3)}}\chi_{(n+1)(l+1)(m-1)}^{\mu}(\mathbf{r},t,\xi,\epsilon_T,\epsilon_P)$$
$$- \sqrt{\frac{(l-m-1)(l-m)}{(2l-1)(2l+1)}}[\chi_{(n+1)(l-1)(m+1)}^{\mu}(\mathbf{r},t,\xi,\epsilon_T,\epsilon_P) - \epsilon_T^2\chi_{(n-1)(l-1)(m+1)}^{\mu}(\mathbf{r},t,\xi,\epsilon_T,\epsilon_P)]$$
$$\left. - \sqrt{\frac{(l+m-1)(l+m)}{(2l-1)(2l+1)}}[\chi_{(n+1)(l-1)(m-1)}^{\mu}(\mathbf{r},t,\xi,\epsilon_T,\epsilon_P) - \epsilon_T^2\chi_{(n-1)(l-1)(m-1)}^{\mu}(\mathbf{r},t,\xi,\epsilon_T,\epsilon_P)]\right),$$

$$z\chi^{\mu}_{nlm}(\mathbf{r},t,\xi,\epsilon_T,\epsilon_P) = \sqrt{\frac{(l-m+1)(l+m+1)}{(2l+1)(2l+3)}}\chi^{\mu}_{(n+1)(l+1)m}(\mathbf{r},t,\xi,\epsilon_T,\epsilon_P) + \sqrt{\frac{(l-m)(l+m)}{(2l-1)(2l+1)}} \times[\chi^{\mu}_{(n+1)(l-1)m}(\mathbf{r},t,\xi,\epsilon_T,\epsilon_P) - \epsilon_T^2\chi^{\mu}_{(n-1)(l-1)m}(\mathbf{r},t,\xi,\epsilon_T,\epsilon_P)], \quad \text{(A10)}$$

which demonstrates explicitly that the application of the laser potential (with any polarization) on a given BGM state can be written as a finite linear combination of BGM states.

[1] *Many-Particle Quantum Dynamics in Atomic and Molecular Fragmentation*, edited by J. Ullrich and V. P. Shevelko (Springer, Heidelberg, 2003).
[2] D. A. Copeland and C. L. Tang, J. Chem. Phys. **65**, 3161 (1976).
[3] M. H. Mittleman, Phys. Rev. A **14**, 586 (1976).
[4] A. Débarre and P. Cahuzac, J. Phys. B **19**, 3965 (1986).
[5] T. Kirchner, Phys. Rev. Lett. **89**, 093203 (2002).
[6] C. Höhr, A. Dorn,T. Alexandrowa, A. Shaheen, C. D. Schröter, R. Moshammer, and J. Ullrich, Abstracts of Contributed Papers to the 23rd International Conference on Photonic, Electronic, and Atomic Collisions (XXIII ICPEAC) (2003).
[7] T. Schmidt, C. Figl, A. Grimpe, J. Grosser, O. Hoffmann, and F. Rebentrost, Phys. Rev. Lett. **92**, 033201 (2004).
[8] S.-M. Li, Y.-G. Miao, Z.-F. Zhou, J. Chen, and Y.-Y. Liu, Z. Phys. D: At., Mol. Clusters **39**, 29 (1997).
[9] S.-M. Li, X.-L. Xu, Z.-F. Zhou, J. Chen, and Y.-Y. Liu, Eur. Phys. J. D **2**, 237 (1998).
[10] S.-M. Li, Y.-G. Miao, Z.-F. Zhou, J. Chen, and Y.-Y. Liu, Phys. Rev. A **57**, 3705 (1998).
[11] A. B. Voitkiv and J. Ullrich, J. Phys. B **34**, 1673 (2001).
[12] A. B. Voitkiv and J. Ullrich, J. Phys. B **34**, 4383 (2001).
[13] S.-M. Li, J. Chen, and Z.-F. Zhou, J. Phys. B **35**, 557 (2002).
[14] L. B. Madsen, J. P. Hansen, and L. Kocbach, Phys. Rev. Lett. **89**, 093202 (2002).
[15] J. P. Hansen, T. Sørevik, and L. B. Madsen, Phys. Rev. A **68**, 031401 (2003).
[16] M. S. Pindzola, T. Minami, and D. R. Schultz, Phys. Rev. A **68**, 013404 (2003).
[17] M. Lein and J. M. Rost, Phys. Rev. Lett. **91**, 243901 (2003).
[18] H. J. Lüdde, A. Henne, T. Kirchner, and R. M. Dreizler, J. Phys. B **29**, 4423 (1996).
[19] O. J. Kroneisen, H. J. Lüdde, T. Kirchner, and R. M. Dreizler, J. Phys. A **32**, 2141 (1999).
[20] H. J. Lüdde, T. Kirchner, and M. Horbatsch, in *Photonic, Electronic, and Atomic Collisions*, edited by J. Burgdörfer, J. Cohen, S. Datz, and C. R. Vane (Rinton Press, Princeton, NJ, 2002), p. 708.
[21] T. G. Winter, Phys. Rev. A **37**, 4656 (1988).
[22] R. Moshammer *et al.*, Phys. Rev. Lett. **84**, 447 (2000).
[23] T. G. Winter and G. J. Hatton, Phys. Rev. A **21**, 793 (1980).
[24] M. B. Shah and H. B. Gilbody, J. Phys. B **11**, 121 (1978).
[25] W. L. Nutt, R. W. McCullough, K. Brady, M. B. Shah, and H. B. Gilbody, J. Phys. B **11**, 1457 (1978).
[26] M. C. van Hemert, E. F. van Dishoeck, J. A. van der Hart, and F. Koike, Phys. Rev. A **31**, 2227 (1985).
[27] L. F. Errea, C. Harel, C. Illescas, H. Jouin, L. Méndez, B. Pons, and A. Riera, J. Phys. B **31**, 3199 (1998).
[28] L. F. Errea, L. Méndez, and A. Riera, J. Chem. Phys. **79**, 4221 (1983).
[29] J. F. Seely, J. Chem. Phys. **75**, 3321 (1981).
[30] T. Niederhausen, B. Feuerstein, and U. Thumm, Abstracts of Contributed Papers to the 23rd International Conference on Photonic, Electronic, and Atomic Collisions (XXIII ICPEAC) (2003).
[31] H. J. Lüdde, in *Many-Particle Quantum Dynamics in Atomic and Molecular Fragmentation* (Ref. [1]), p. 205.
[32] T. Kirchner, in *Many-Particle Quantum Dynamics in Atomic and Molecular Fragmentation* (Ref. [1]), p. 447.
[33] W. Magnus, F. Oberhettinger, and R. P. Soni, *Formulas and Theorems for the Special Functions of Mathematical Physics* (Springer, Berlin, 1966).